SIEMENS

usa.siemens.com/healthcare

Advancing Diffusion MRI Using Simultaneous Multi-Slice Echo Planar Imaging

Kawin Setsompop, Stephen F. Cauley, Lawrence L. Wald

Advancing Diffusion MRI Using Simultaneous Multi-Slice Echo Planar Imaging

Kawin Setsompop[1, 2]; Stephen F. Cauley[1, 2]; Lawrence L. Wald[1, 2]

[1] Martinos Center for Biomedical Imaging, Department of Radiology, Massachusetts General Hospital, Charlestown, MA, USA
[2] Department of Radiology, Harvard Medical School, Boston, MA, USA

Introduction

There has been a recent significant interest in the use of parallel imaging based Simultaneous Multi-Slice (SMS) acquisition [1] to increase the temporal efficiency of many imaging sequences in MRI. In particular, the use of SMS for diffusion MRI (dMRI) and functional MRI (fMRI) has fundamentally changed the scope of studies that clinicians and researchers are able to perform with these imaging sequences. For dMRI, SMS has opened up the possibility of obtaining information from many more diffusion encoding directions in a limited timeframe, to enable more complex/advanced diffusion acquisitions to be performed in clinical and neuroscientific settings.

Due to the use of diffusion encoding gradients in dMRI, large temporally and spatially varying phase contamination exists, which hampers the utility of multi-shot acquisitions. As such, dMRI acquisitions are often based on rapid single-shot 2D spin-echo EPI sequence. This sequence provides high quality imaging but at a cost of being highly inefficient. Figure 1 shows the sequence diagram for such acquisition, where a single 2D imaging slice is excited, after which diffusion encoding is performed and the data for that particular slice is then readout/received using EPI encoding. This process is repeated multiple times, once for each imaging slice, until whole-brain coverage is achieved. As depicted, the diffusion encoding period can represent a significant portion of the acquisition time. This diffusion encoding is performed using magnetic field gradient pulses which provide encoding to the whole imaging volume. However, for each acquisition period, only a single slice is excited and acquired, and the lengthy diffusion encoding has to be repeated for all imaging slices, leading to large inefficiency.

1

Standard 2D slice-by-slice dMRI

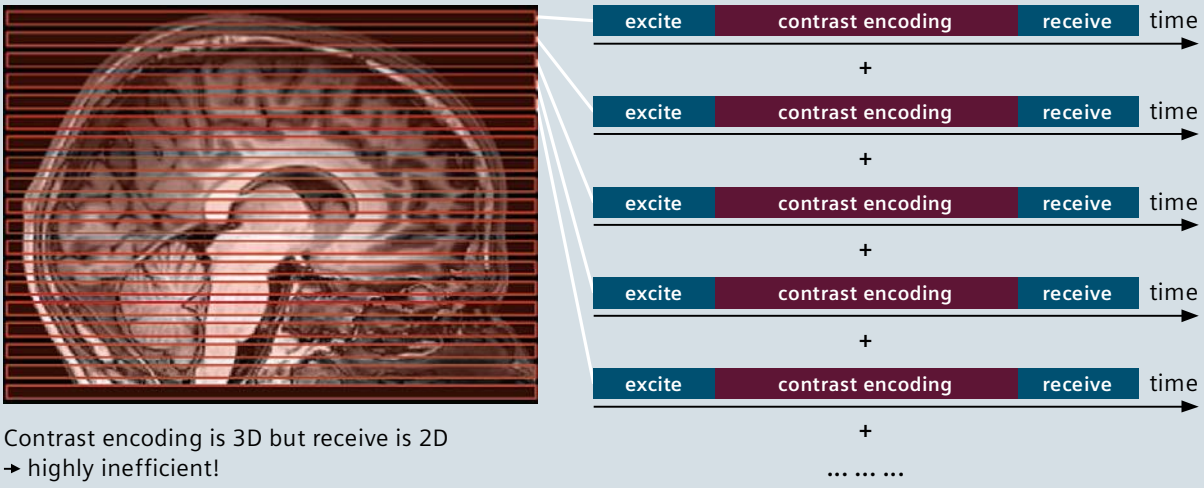

Contrast encoding is 3D but receive is 2D
→ highly inefficient!

1 The inefficiency of standard 2D DWI techniques is illustrated. Although the lengthy diffusion contrast-encoding encompasses the entire volume, only a single slice is acquired. Simultaneous multi-slice enables the concurrent acquisition of several imaging slices during a single diffusion encoding. Unlike typical in-plane acceleration techniques, which only shorten the receive portion of the acquisition, SMS allows for proportional reductions in total scan time as the multiband factor is increased.

The use of conventional 2D parallel imaging acceleration [2-4] in dMRI can reduce the number of phase encoding steps of EPI which reduces image distortion and blurring artifacts. However, such technique does not provide significant acceleration to dMRI, since they only shorten the EPI encoding period and not the other components of the data acquisition, in particular the lengthy diffusion encoding. The use of simultaneous multi-slice (SMS) acceleration [1], on the other hand, allows for the concurrent acquisition of several imaging slices (the slices will appear collapsed before reconstruction) during each acquisition period, thereby reducing the number of acquisition periods needed to perform volumetric acquisition. Thus, SMS is much more effective at providing scan time reduction in dMRI, where the total scan time is now reduced by a factor equal to the number of simultaneously excited slices (multiband (MB) factor). Additionally, unlike conventional parallel imaging, SMS does not shorten the EPI encoding period and is not affected by the undesirable $\sqrt{R}$ SNR penalty of conventional parallel imaging.

Several SMS methods have been applied to single shot SMS-EPI, including Wideband imaging [5, 6], Simultaneous Image Refocusing (SIR) [7, 8] and parallel image reconstruction based multi-slice imaging [9, 10]. However, the presence of significant artifact and/or signal-to-noise (SNR) loss from these methods have prevented their wide scale adoption in dMRI. In particular, parallel imaging based multi-slice imaging suffers from high *g*-factor noise amplification in brain MRI. This is due to the fact that the imaging field-of-view (FOV) along the slice direction is typically small for brain acquisitions, causing the aliased voxels of the simultaneously acquired slices to be spatially close which makes it hard to tease them apart. An improved parallel imaging strategy termed CAIPIRINHA [11], which creates an inter-slice image shift between simultaneously acquired slices to increase the distance between the aliased voxels has been proposed as a way to reduce the *g*-factor penalty associated with SMS. The CAIPIRINHA method creates an inter-slice shift by utilizing a different RF pulse for the data acquisition of each *k*-space line, where each RF pulse is designed to induce a different phase modulation to each of the slices that are being acquired simultaneously. This is feasible for multi-shot acquisitions but not for single-shot EPI where only a single RF pulse is used to acquire all lines of *k*-space. An initial attempt to adopt CAIPIRINHA for single-shot EPI acquisitions was performed by Nunes *et al*. [9]. Here, a Wideband-like approach was used in the phase encoding and readout directions to increase the distance between aliased voxels. However, this resulted in voxel tilting (blurring) artifacts and heavily restricted the distance that could be imposed between aliased voxels. In this article, we describe the blipped-CAIPIRINHA method [12] which is a modification of Nunes' approach, to generate the desired voxel shifts in the phase encoding direction without tilting artifacts. This approach has provided us with the ability to perform high quality parallel imaging based SMS-EPI acquisition that can be used to significantly shorten dMRI acquisition time.

Blipped-CAIPIRINHA

The blipped-CAIPIRINHA method utilizes additional G_z magnetic field gradient blips during the EPI readout. Figure 2 shows the standard G_x and G_y gradients of the EPI encoding, along with these additional G_z gradient blips. These G_z blips are applied concurrently with the G_y phase encoding blips to create a different phase modulation between the simultaneously excited slices for the data acquisition of each *k*-space line. For this example, the G_z blips are being applied to create a FOV/2 shift along the phase encoding (PE) direction between two simultaneously acquired slices (collapsed image shown in top-right of Figure 2). In order to create the desired inter-slice shift, an appropriate gradient blip area must be used for these G_z blips. Specifically, in the example in

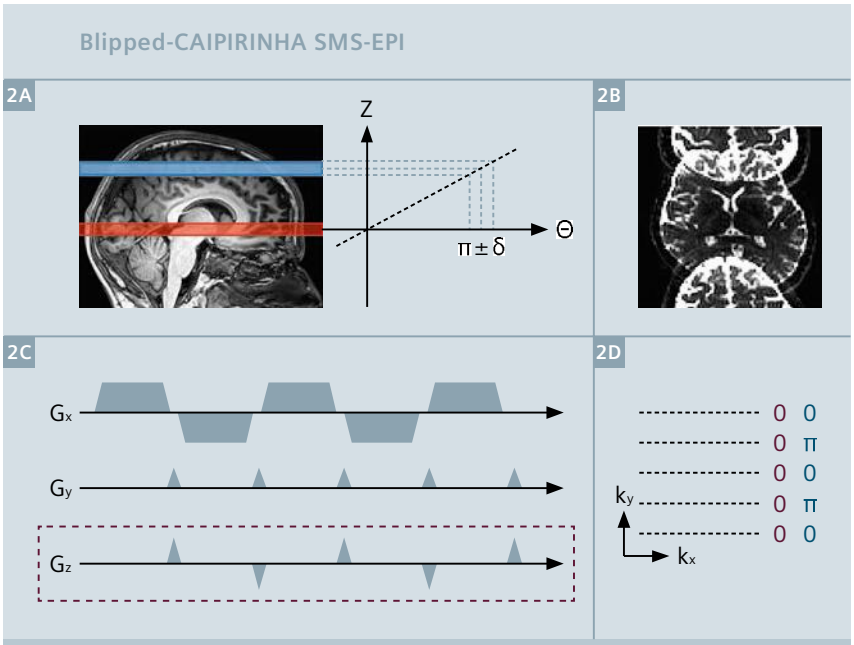

2 A blipped-CAIPIRINHA SMS-EPI gradient scheme applied across the X, Y and Z (Readout, Phase-Encode, and Slice) axes is illustrated. The G_z gradient blips required to create a FOV/2 shift between two simultaneously acquired slices are shown (collapsed image in **2B**). The blipped-CAIPIRINHA method varies the sign of the G_z gradient blips in order to avoid accumulation of through-slice phase variation, which would result in voxel titling artifacts. The accumulated phase applied to each of the k_y lines are shown for the two slices **(2D).**

Figure 2, each G_z blip will have to create a π phase increment to the spins located at the upper slice (blue) and no increment to the lower slice (red). The phase modulations along k_y caused by the G_z blip train are shown on the lower-right of Figure 2, for the upper (blue) and lower (red) imaging slices. With no phase modulation to the lower slice, this slice remains unaffected. On the other hand, the linear phase moduation along k_y at π phase increment for the top slice causes this slice to shift by FOV/2 along the PE direction. As such, a desired FOV/2 inter-slice shift is achieved.

It is important to note that each G_z blip will also introduce a small phase variation 2δ across the finitely thick slices being acquired as shown in Figure 2. This through-slice phase variation created by each blip will result in a very minor signal attenuation (typically less than 1%).
The important concept in blipped-CAIPIRINHA is the utilization of alternating positive and negative gradient blips to limit ability of the gradient moment and this through-slice phase variation to accumulate during the EPI encode and cause significant signal attenuation. This solves the issue of the Wideband approach where only positive G_z blips are employed which results in accumulation of through-slice dephasing and voxel tilting artifacts. Thus, the blipped-CAIPIRINHA method facilitates efficient CAIPIRINHA controlled aliasing schemes for simultaneously acquired slices in EPI. This can be seen clearly when examining the 3× slice-accelerated (SMS 3) example acquired using a 32-channel head coil at 3T shown in Figure 3. Here, the *g*-factor associated with FOV/2 shift and no-shift parallel imaging reconstructions are compared (both with slice-GRAPPA reconstruction). When no-shift was applied between the simultaneously acquired slices, the average retained SNR (1 / *g*-factor) dropped significantly to 68%. The blipped-CAIPIRINHA method with FOV/2 shift retained over 99% of the SNR, while removing the 3.5 voxel tilt that would have been present with the standard wideband approach. Thereby, blipped-CAIPIRINHA enables three times faster acquisitions in dMRI without incurring significant SNR penalty. (Note that in some regions the retained SNR is slightly greater than unity indicating some noise cancellation in the reconstruction process as previously demonstrated in low acceleration in-plane GRAPPA acquisitions [13]).

3 SMS-3 Blipped-CAIPIRINHA with 32-channel head coil

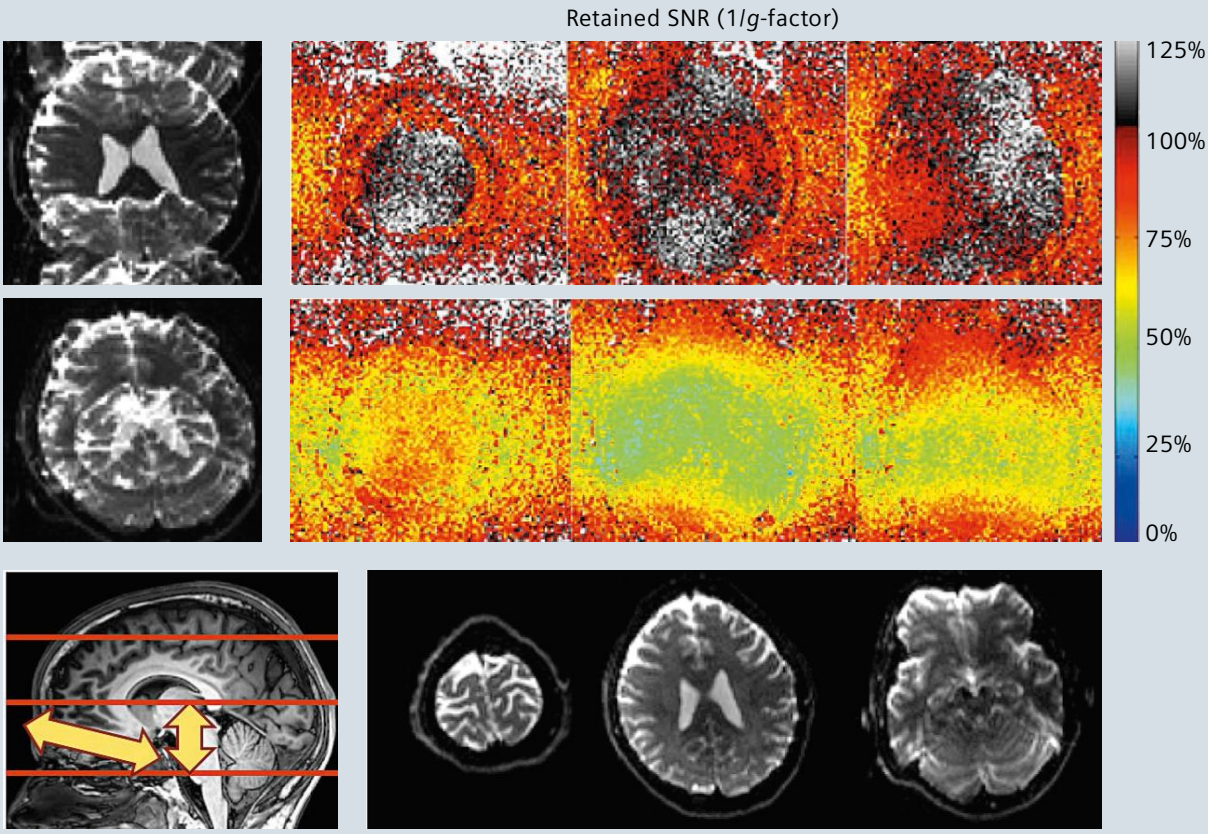

3 SMS-EPI at SMS-3 acceleration acquired at 3T using Siemens' 32-channel coil. The *g*-factor associated with FOV/2 shift and no-shift parallel imaging reconstructions are compared. The retained SNR (1 / *g*-factor), when no-shift was applied dropped significantly to 68%. The blipped-CAIPIRINHA method with FOV/2 shift retained over 99% of the SNR, while avoiding the 3.5 voxel tilt associated with standard wideband approaches.

RF pulse design and image reconstruction

When considering the use of blipped-CAIPIRINHA for high slice acceleration factors, there are several sequence design and image reconstruction aspects that need to be carefully developed. Of particular importance to diffusion-weighted imaging (DWI) is the design of the multiband RF pulse that allows for multiple slices to be simultaneously excited in SMS acquisitions. Multiband RF pulses cause an increase in SAR, which is especially problematic for DWI since it relies on high SAR spin-echo 90-180 pulses. At SMS-3 acceleration, the use of the VERSE algorithm [14] has been shown to provide adequate SAR reduction for *in vivo* DWI at 3T [15]. However, the benefit of SAR reduction from VERSE comes at a cost of slice profile distortion at off-resonance frequencies. This can be mitigated by the use of the SLR algorithm for RF pulse design along with a high time-bandwidth product that improves the slice-profile quality prior to the application of VERSE. Figure 4 (A, B) shows multiband 90-180 pulses with slice acceleration factor 3 designed using both the SLR and VERSE algorithms. Figure 4A shows the VERSE 90 and 180 RF pulses along with corresponding gradient pulses. Figure 4B shows the comparison of slice-profiles obtained from a standard single-slice 90-180 RF pulse pair and those obtained from the slice acceleration factor 3 RF pulse pair. Here, the high-quality slice profiles are achieved at both on resonance and 50 Hz off-resonance.

In addition to the combined design of VERSE and SLR, a number of other approaches have been developed to reduce both SAR and peak-power of MB pulses. These techniques are particularly beneficial at higher slice accelerations and/or for ultra-high field imaging. In order to reduce peak-power, a phase optimization scheme [16], a pulse time-shift method [17] and a combined approach [18, 19] of phase optimization with the use of 90° and 180° pulses with spatially-varying phases that combine to provide a flat spin-echo excitation phase have been

Multiband RF pulse: SLR & VERSE algorithm

high quality slice profile and low SAR

4A

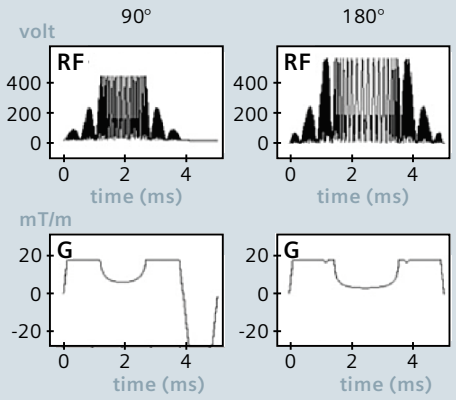

4B

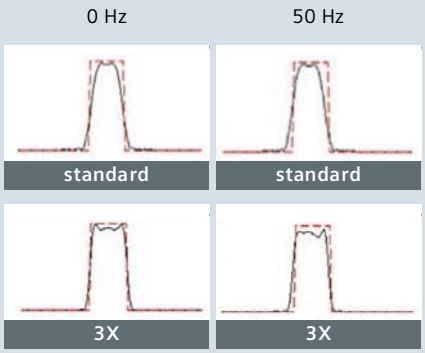

Slice-GRAPPA recon: leak-block and dual kernel

4C

Reduced signal leakage between slices

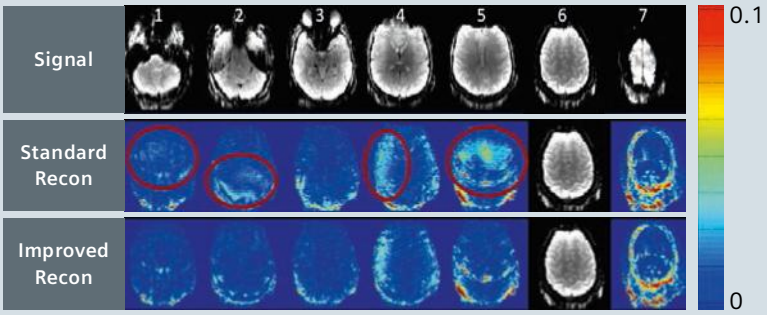

4D

Reduced N/2 ghost level

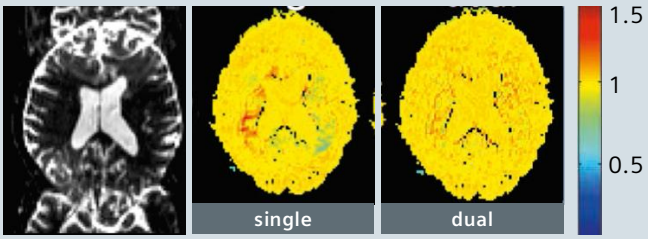

4 Critical implementation aspects for the blipped-CAIPIRINHA method are highlighted. The multiband 90-180 pulses with slice acceleration factor-3 designed using both the SLR and VERSE algorithms are shown. **(4A)** The VERSE 90 and 180 RF pulses along with corresponding Gradient pulses. **(4B)** A comparison of slice-profiles from a standard single-slice 90-180 RF pulse pair and those obtained from the slice acceleration factor 3 RF pulse pair. These pulses are necessary to ensure image quality while limiting peak-power and SAR. The benefits of the 'LeakBlock' Slice-GRAPPA reconstruction technique in reducing leakage signal contamination between simultaneously acquired slices is shown **(4C)**.The individual leakage signal contaminations onto the 6th imaging slice (for a SMS 7 acquisition) are greatly reduced when compared with standard slice-GRAPPA reconstruction. The use of 'dual kernel' slice-GRAPPA to separate SMS 3 blipped-CAIPIRINHA EPI with FOV/2 shift data is shown **(4D)**. The dual kernels operate specifically to the even and the odd lines of the slice-collapsed *k*-space data, and enable clean separation of both of the slice data and associated ghost (prior to the application of typical ghost correction).

proposed. In addition, the Power Independent of Number of Slices (PINS) [20] and MultiPINS [21] RF pulse designs have been proposed as a strategy to excite/refocus a large number of imaging slices simultaneously without increasing peak power or SAR.

A number of techniques have been developed in order to improve the quality of SMS-EPI image reconstruction. The original SENSE/GRAPPA approach for SMS reconstruction [22] has been modified to facilitate CAIPIRINHA acquisitions with inter-slice FOV shifts [23-25]. Slice-GRAPPA [12], which has been widely-used for blipped-CAIPIRINHA SMS-EPI reconstruction, has been redesigned to provide robust reconstruction through a 'LeakBlock' technique [26]. This technique reduces the leakage signal contamination between simultaneously acquired slices and has been shown to improve temporal stability at high accelerations. Figure 4C shows a comparison of signal leakage contamination in the standard and the improved LeakBlock slice-GRAPPA reconstructions for blipped-CAIPIRINHA acquisition at SMS-7 using a 32-channel head coil. It can be clearly seen that the individual leakage signal contaminations onto the 6th imaging slice are greatly reduced using the LeakBlock reconstruction.

Another important consideration for SMS-EPI reconstruction is in the minimization of N/2 image ghosting artifacts. For SMS-EPI, this is a particular concern since a different slice-specific ghost correction could be required for each of the simultaneously acquired imaging slices (due to differences in phase error of the N/2 ghost for different slice locations). Thus, the N/2 ghost cannot be cleanly removed from the slice-collapsed dataset prior to the parallel imaging (slice-unaliasing) reconstruction. The use of a 'dual kernel' slice-GRAPPA, where separate GRAPPA kernels are applied to the even and the odd lines of the slice-collapsed *k*-space data has been shown to overcome this issue [15]. This method enables a clean separation of both of the slice data and associated ghost, prior to the application of typical ghost correction.

Figure 4D shows a comparison of the N/2 ghost artifact level for an SMS-3 blipped-CAIPIRINHA SMS-EPI with FOV/2 shift reconstructed using i) single kernel slice-GRAPPA and ii) dual kernel slice-GRAPPA approaches. Note that the ghost artifact of the top imaging slice in the SMS acquisition lands directly in the center of the imaging FOV of the middle imaging slice (due to the FOV/2 inter-slice shift). This prevents the single kernel slice-GRAPPA approach from accurately unaliasing the ghosting artifact. Figure 4 shows the corresponding large reconstruction artifact in the center of the middle imaging slice. With the use of dual kernel slice-GRAPPA, this artifact has been mitigated. The dual kernel approach has been successfully applied to SENSE/GRAPPA reconstruction [27] and an extension of the method has been used to overcome artifacts associated with phase-encode line bunching [28]. Finally, for SENSE based reconstruction of SMS data, a slice-specific phase error of the ghost artifact has been successfully incorporated into the parallel imaging reconstruction [29].

Diffusion-weighted imaging applications

With the careful design of RF pulses and the image reconstruction framework, blipped-CAIPIRINHA allows for the efficient acquisition of high quality SMS-EPI data for DWI. In clinical settings, where time is limited, DWI is often restricted to only a small number of diffusion encoding directions. This constrains studies to only examine the most basic diffusion information, such as the apparent diffusion coefficient (ADC). With the use of blipped-CAIPIRINHA SMS-EPI, diffusion-weighted acquisitions can be accelerated robustly by 3-fold to provide high quality data with negligible SNR loss and artifact levels. This has allowed for more diffusion directions to be obtained in a clinically relevant time-frame, enabling more complex diffusion models/metrics (e.g. Fractional Anisotropy (FA), Diffusion Kurtosis, and fiber tracking) to be considered. Figure 5 demonstrates the use of blipped-CAIPIRINHA to achieve 3-fold acceleration for typical neuroimaging acquisitions based upon Diffusion Tensor Imaging (DTI), Q-ball, and Diffusion Spectrum Imaging (DSI). Here, the color FA, Orientation Distribution Function (ODF), and the fiber tracking results from these diffusion models are compared using standard SMS-1 and blipped-CAIPIRINHA SMS-3 acquisitions. In all cases, the high quality of the results is maintained at a 3-fold speed up with the blipped-CAIPIRINHA technique.

There is a growing interest in the application of DWI to areas outside the brain, where it has also proven to be highly sensitive to tissue abnormalities. Similar to the neuroimaging applications described above, blipped-CAIPIRINHA SMS-EPI can play a role in speeding up acquisitions in the body. Here, a large in-plane FOV has to be encoded and in-plane acceleration (typically a factor of 2) is used to reduce image distortion. While accelerations in the slice and in-plane directions are compatible, the use of both can lead to a high total acceleration factor (the product of the two acceleration factors) and result in higher *g*-factor noise amplifications. For the DWI applications where SNR is inherently low, it is desirable to keep the noise penalty to a minimum. Thus, a combined SMS-2 and in-plane-2 acceleration strategy is typically employed for blipped-CAIPIRINHA SMS-EPI in the body.

Figure 6 shows DWI results for liver, whole-body, and breast imaging from a standard in-plane-2 acceleration with and without the inclusion of blipped-CAIPIRINHA SMS factor 2. The imaging results are near identical, with the blipped-CAIPIRINHA acquisition providing a 2-fold speed up in imaging time. This is particularly useful for whole-body DWI, where a large number of imaging slices are acquired. Reducing these lengthy scans (often ~20 minutes is required for standard diffusion scans focusing on the basic ADC metric) will have a significant impact on the wide-spread adoption of whole-body DWI in clinical settings.

5

3x Faster brain dMRI

Q-ball: 12 min → 4 min

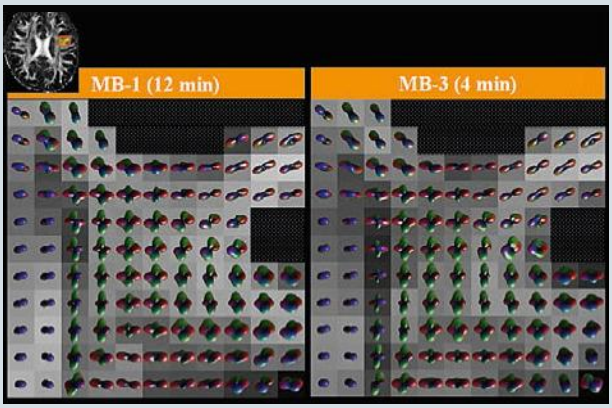

DTI: 10 min → 3 min

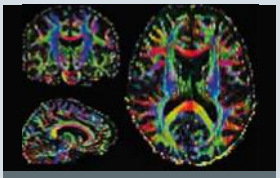

1x Aquisition

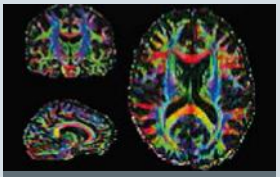

3x Aquisition

DSI: 45 min → 15 min

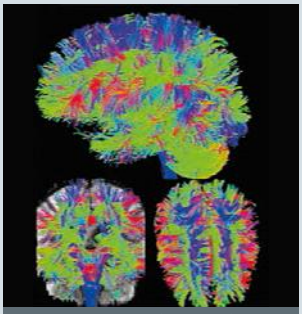

MB-1 DSI (45 min)

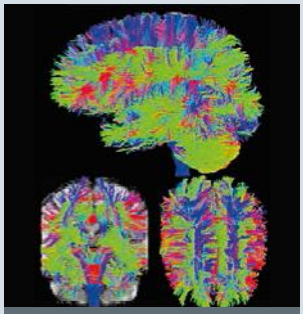

MB-3 DSI (15 min)

5 Diffusion Tensor Imaging, Q-ball, and Diffusion Spectrum Imaging are compared using standard SMS 1 and blipped-CAIPIRINHA SMS 3 acquisitions at 3T using Siemens' 32-channel head coil. The high level of similarities in color FA, Orientation Distribution Function, and the fiber tracking results can be clearly seen.

6

Applications outside of the brain

Liver diffusion

b = 50

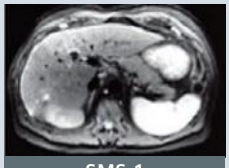

SMS-1

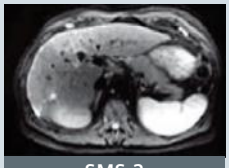

SMS-2

b = 400

SMS-1

SMS-2

b = 800

SMS-1

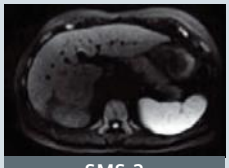

SMS-2

ADC

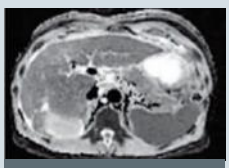

SMS-1

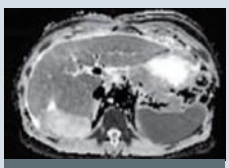

SMS-2

Whole-body diffusion

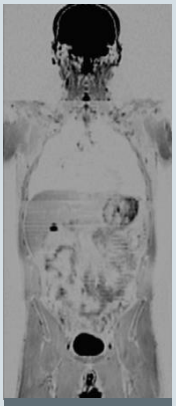

SMS-1

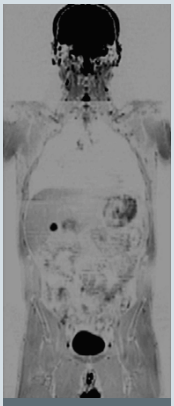

SMS-2

Breast diffusion

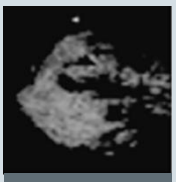

SMS-1

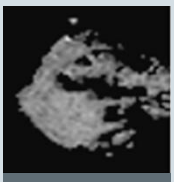

SMS-2

6 Emerging applications of DWI in the body are demonstrated. Blipped-CAIPIRINHA with SMS 2 and in-plane GRAPPA 2 was used in large FOV body diffusion. Relative to conventional DWI with in-plane GRAPPA 2, similar image quality can be seen. Blipped-CAIPIRINHA SMS enables effective combination of in-plane GRAPPA acceleration which is critical for the reduction of distortions especially in large FOV DWI of the body. With blipped-CAIPIRINHA SMS-EPI, scan time reductions to a factor of 2 with similar image quality can be obtained for the liver, breast, and whole-body DWI.

References

1 Larkman DJ, Hajnal J V, Herlihy AH, Coutts GA, Young IR, Ehnholm G. Use of multicoil arrays for separation of signal from multiple slices simultaneously excited. J Magn Reson imaging. 2001;13:313–7.

2 Pruessmann KP, Weiger M, Scheidegger MB, Boesiger P. SENSE: sensitivity encoding for fast MRI. Magn Reson Med [Internet]. 1999 Nov;42(5):952–62. Available from: 10.1002/(SICI)1522-2594(199911)42:5<952::AID-MRM16>3.0.CO;2-S.

3 Griswold MA, Jakob PM, Heidemann RM, Nittka M, Jellus V, Wang J, et al. Generalized autocalibrating partially parallel acquisitions (GRAPPA). Magn Reson Med [Internet]. 2002 Jun [cited 2014 Jan 21];47(6):1202–10. Available from: http://www.ncbi.nlm.nih.gov/pubmed/12111967.

4 Sodickson DK, Manning WJ. Simultaneous acquisition of spatial harmonics (SMASH): fast imaging with radiofrequency coil arrays. Magn Reson Med [Internet]. 1997 Oct;38(4):591–603. Available from: http://www.ncbi.nlm.nih.gov/pubmed/9324327.

5 Paley MNJ, Lee KJ, Wild JM, Griffiths PD, Whitby EH. Simultaneous parallel inclined readout image technique. Magn Reson Imaging [Internet]. 2006 Jun [cited 2014 Sep 9];24(5):557–62. Available from: http://www.ncbi.nlm.nih.gov/pubmed/16735176.

6 Weaver JB. Simultaneous Multislice Acquisition of MR Images. 1988;284:275–84.

7 Feinberg D a., Reese TG, Wedeen VJ. Simultaneous echo refocusing in EPI. Magn Reson Med. 2002;48(1):1–5.

8 Reese TG, Benner T, Wang R, Feinberg D a., Van Wedeen J. Halving imaging time of whole brain diffusion spectrum imaging and diffusion tractography using simultaneous image refocusing in EPI. J Magn Reson Imaging. 2009;29(3):517–22.

9 Nunes RG, Hajnal J V, Golay X, Larkman DJ. Simultaneous slice excitation and reconstruction for single shot EPI . Proc Intl Soc Mag Reson Med. 2006. p. 293.

10 Moeller S, Yacoub E, Olman C a, Auerbach EJ, Strupp J, Harel N, et al. Multiband multislice GE-EPI at 7 tesla, with 16-fold acceleration using partial parallel imaging with application to high spatial and temporal whole-brain fMRI. Magn Reson Med [Internet]. 2010 May [cited 2014 Jan 21];63(5):1144–53. Available from: http://www.pubmedcentral.nih.gov/articlerender.fcgi?artid=2906244&tool=pmcentrez&rendertype=abstract.

11 Breuer FA, Blaimer M, Heidemann RM, Mueller MF, Griswold MA, Jakob PM. Controlled aliasing in parallel imaging results in higher acceleration (CAIPIRINHA) for multi-slice imaging. Magn Reson Med. 2005;53:684–91.

12 Setsompop K, Gagoski BA, Polimeni JR, Witzel T, Wedeen VJ, Wald LL. Blipped-controlled aliasing in parallel imaging for simultaneous multislice echo planar imaging with reduced g-factor penalty. Magn Reson Med [Internet]. 2012 May [cited 2014 Jan 21];67(5):1210–24. Available from: http://www.pubmedcentral.nih.gov/articlerender.fcgi?artid=3323676&tool=pmcentrez&rendertype=abstract.

13 Polimeni JR, Wiggins GC, Wald LL. Characterization of artifacts and noise enhancement introduced by GRAPPA reconstructions. Proc Intl Soc Mag Reson Med. 2008. p. 1286.

14 Conolly SM, Nishimura DG, Macovski A, Glover GH. Variable-rate selective excitation. J Magn Reson [Internet]. 1988 Jul [cited 2012 Jul 4];78(3):440–58. Available from: http://linkinghub.elsevier.com/retrieve/pii/002223648890131X.

15 Setsompop K, Cohen-Adad J, Gagoski BA, Raij T, Yendiki A, Keil B, et al. Improving diffusion MRI using simultaneous multi-slice echo planar imaging. Neuroimage [Internet]. Elsevier Inc.; 2012 Oct 15 [cited 2014 Jan 30];63(1):569–80. Available from: http://www.pubmedcentral.nih.gov/articlerender.fcgi?artid=3429710&tool=pmcentrez&rendertype=abstract.

16 Wong E. Optimized phase schedules for minimizing peak RF power in simultaneous multi-slice RF excitation pulses. Proc Intl Soc Mag Reson Med [Internet]. 2012 [cited 2014 Jan 21]. p. 2209. Available from: http://scholar.google.com/scholar?hl=en&btnG=Search&q=intitle:Optimized+phase+schedules+for+minimizing+peak+RF+power+in+simultaneous+multi-slice+RF+excitation+pulses#0.

17 Auerbach EJ, Xu J, Yacoub E, Moeller S, Uğurbil K. Multiband accelerated spin-echo echo planar imaging with reduced peak RF power using time-shifted RF pulses. Magn Reson Med. 2013 May;69(5):1261–7.

18 Zhu K, Kerr AB, Pauly JM. Nonlinear-Phase Multiband 90°-180° RF Pair With Reduced Peak Power. Proc Intl Soc Mag Reson Med. 2014. p. 1440.

19 Sharma A, Bammer R, Stenger VA, Grissom W a. Low peak power multiband spokes pulses for B 1 + inhomogeneity-compensated simultaneous multislice excitation in high field MRI. Magn Reson Med [Internet]. 2015;doi: 10.1002/mrm.25455. Available from: http://doi.wiley.com/10.1002/mrm.25455.

20 Norris DG, Koopmans PJ, Boyacioğlu R, Barth M. Power Independent of Number of Slices (PINS) radiofrequency pulses for low-power simultaneous multislice excitation. Magn Reson Med [Internet]. 2011 Nov [cited 2014 Jan 10];66(5):1234–40. Available from: http://www.ncbi.nlm.nih.gov/pubmed/22009706.

21 Eichner C, Wald LL, Setsompop K. A low power radiofrequency pulse for simultaneous multislice excitation and refocusing. Magn Reson Med [Internet]. 2014 Oct [cited 2014 Sep 25];72:949–58. Available from: http://www.ncbi.nlm.nih.gov/pubmed/25103999.

22 Blaimer M, Breuer F a, Seiberlich N, Mueller MF, Heidemann RM, Jellus V, et al. Accelerated volumetric MRI with a SENSE/GRAPPA combination. J Magn Reson imaging [Internet]. 2006 Aug [cited 2014 Oct 13];24(2):444–50. Available from: http://www.ncbi.nlm.nih.gov/pubmed/16786571.

23 Stäb D, Ritter CO, Breuer F a, Weng AM, Hahn D, Köstler H. CAIPIRINHA accelerated SSFP imaging. Magn Reson Med. 2011;65:157–64.

24 Blaimer M, Choli M, Jakob PM, Griswold M a, Breuer F a. Multiband phase-constrained parallel MRI. Magn Reson Med [Internet]. 2013 Apr [cited 2014 Jul 21];69(4):974–80. Available from: http://www.pubmedcentral.nih.gov/articlerender.fcgi?artid=3606646&tool=pmcentrez&rendertype=abstract.

25 Moeller S, Vu AT, Auerbach E, Ugurbil K, Yacoub E. RO extended FOV SENSE/GRAPPA for multiband imaging with FOV shift. Proc Intl Soc Mag Reson Med. 2014. p. 4396.

26 Cauley SF, Polimeni JR, Bhat H, Wald LL, Setsompop K. Interslice leakage artifact reduction technique for simultaneous multislice acquisitions. Magn Reson Med [Internet]. 2014 [cited 2014 Jan 28];72:93–102. Available from: http://www.ncbi.nlm.nih.gov/pubmed/23963964.

27 Koopmans PJ, Poser BA, Breuer FA. 2D-SENSE-GRAPPA For Fast, Ghosting-Robust Reconstruction of In-Plane and Slice Accelerated Blipped-CAIPI-EPI. Proc Intl Soc Mag Reson Med. 2015. p. 2410.

28 Moeller S, Auerbach EJ, Vu AT, Lenglet C, Sotiropoulos SN, Ugurbil K, et al. EPI 2D ghost correction and integration with multiband : application to diffusion imaging at 7T. Proc Intl Soc Mag Reson Med. 2015. p. 248.

29 Zhu K, Dougherty RF, Takahashi A, Pauly J, Kerr AB. Nyquist Ghosting Correction For Simultaneous Multislice Echo Planar Imaging. 2014. p. 647.

Contact

Kawin Setsompop
Massachusetts General Hospital
Martinos Center for Biomedical Imaging
Building 75, Room 2.102, 13th Street
Charlestown, MA, 02129, USA
Phone: +1 617-669-6640
kawin@nmr.mgh.harvard.edu

The outcomes achieved by the Siemens customers described herein were achieved in the customers' unique setting. Since there is no "typical" hospital and many variables exist, there can be no guarantee that others will achieve the same results.

On account of certain regional limitations of sales rights and service availability, we cannot guarantee that all products included in this brochure are available through the Siemens sales organization worldwide. Availability and packaging may vary by country and is subject to change without prior notice. Some/All of the features and products described herein may not be available in the United States.

The information in this document contains general technical descriptions of specifications and options as well as standard and optional features, which do not always have to be present in individual cases.

Siemens reserves the right to modify the design, packaging, specifications, and options described herein without prior notice. Please contact your local Siemens sales representative for the most current information.

Note: Any technical data contained in this document may vary within defined tolerances. Original images always lose a certain amount of detail when reproduced.

Local Contact Information
Siemens Medical Solutions USA, Inc.
40 Liberty Boulevard
Malvern, PA 19355-9998
USA
Phone: +1-888-826-9702
usa.siemens.com/healthcare

Siemens Healthcare Headquarters
Siemens Healthcare GmbH
Henkestr. 127
91052 Erlangen
Germany
Phone: +49 9131 84-0
siemens.com/healthcare

Legal Manufacturer
Siemens Healthcare GmbH
Henkestr. 127
91052 Erlangen
Germany

Order No. A91DI-MR-16944-P1-4A00 | Printed in USA 04-2016 |

siemens.com/healthcare